Published online 9 July 2020

Nucleic Acids Research, 2020, Vol. 48, No. 15 ***8591–8600***
doi: 10.1093/nar/gkaa581

Switching the activity of Taq polymerase using clamp-like triplex aptamer structure

Yingxin Hu [1,2], Zhiyu Wang[1], Zhekun Chen[1] and Linqiang Pan [1,*]

[1]Key Laboratory of Image Information Processing and Intelligent Control of Education Ministry of China, School of Artificial Intelligence and Automation, Huazhong University of Science and Technology, Wuhan, Hubei 430074, China and [2]College of Information Science and Technology, Shijiazhuang Tiedao University, Shijiazhuang, Hebei 050043, China

Received April 08, 2020; Revised May 31, 2020; Editorial Decision June 22, 2020; Accepted June 27, 2020

ABSTRACT

In nature, allostery is the principal approach for regulating cellular processes and pathways. Inspired by nature, structure-switching aptamer-based nanodevices are widely used in artificial biotechnologies. However, the canonical aptamer structures in the nanodevices usually adopt a duplex form, which limits the flexibility and controllability. Here, a new regulating strategy based on a clamp-like triplex aptamer structure (CLTAS) was proposed for switching DNA polymerase activity via conformational changes. It was demonstrated that the polymerase activity could be regulated by either adjusting structure parameters or dynamic reactions including strand displacement or enzymatic digestion. Compared with the duplex aptamer structure, the CLTAS possesses programmability, excellent affinity and high discrimination efficiency. The CLTAS was successfully applied to distinguish single-base mismatches. The strategy expands the application scope of triplex structures and shows potential in biosensing and programmable nanomachines.

INTRODUCTION

Allostery is the primary method that regulates cellular processes and pathways in nature (1). Taking inspiration from nature, structure-switching nanodevices are widely employed in artificial biotechnologies and DNA nanotechnology (2–4). Due to its nucleic acid characteristic, aptamer has become a fascinating element for designing structure-switching nanodevices and a variety of applications ranging from biosensing to disease diagnosis and treatment had emerged (2,5–11). Moreover, many efforts have been devoted to the exploration of strategies of integrating enzymes into the aptamer-based nanodevices. For instance, an aptamer-based approach has been proposed to regulate DNA polymerase activity (12–15) and this approach has also been employed in biosensing to detect target DNA (14), protein (16–18), enzymes (19,20), as well as in constructing molecular circuits (21). However, the canonical aptamer structures in use usually adopt a duplex form, which limits the application of enzyme owing to deficiency of a programmable and controllable regulation of enzyme activity. Thereby, the development of a strategy to regulate the polymerase activity in a programmable, controllable, and flexible manner is essential for constructing aptamer-based nanodevices.

Recently, the triplex structure has drawn broad attention from researchers and has become a powerful and alternative motif in the design of structure-switching nanodevices, which introduces a novel paradigm into DNA engineering (22–24). Compared with classical double-helix structures, triplex structures contain C–G•C+ and T–A•T base pairs, in which Watson−Crick base pairs and Hoogsteen interactions synergistically regulate binding strength (22). These triplexes are unique in their pH responsiveness, structural tunability, and versatility, which offer elaborate controllability for bonding strength. Meanwhile, triplex structures can influence biological processes such as gene translation, DNA transcription, replication, and cleavage (25,26). Due to the unique characteristic of triplex structures, they have been reported to have applications in a variety of DNA-related fields, including gene regulation (25,27), biosensors (28–31), nano switches (32–37), nanomachines (38–43), nanostructures (44,45), and target-responsive systems (32,46–49). Despite these achievements, it is imperative for DNA triple helixes to expand their applications. Considering the characteristics of the triplex and aptamer, it is meaningful to combine the triple helical structure with the aptamer to construct nanodevices in a programmable, controllable, and flexible manner, which will expand the toolbox of DNA nanotechnology.

Herein, we devised a clamp-like triplex aptamer structure (CLTAS) to regulate Taq polymerase activity. The CLTAS combines an aptamer sequence that recognizes the poly-

*To whom correspondence should be addressed. Tel: +86 27 87556070; Fax: +86 27 87543130; Email: lqpan@mail.hust.edu.cn

merase and the triplex-forming recognition component into an open clamp structure. Upon binding to a sequence-specific DNA target through Watson–Crick and Hoogsteen base pairings, the formation of the triplex structure changes the CLTAS from an open state to a closed state. The closed CLTAS has an inhibitory capability against polymerase. Using this strategy, Taq polymerase activity can be modulated by reconfiguring the triplex structure. As a demonstration of the strategy, DNA strand displacement and nicking-enzyme digestion were employed to change the conformation of the CLTAS and regulate Taq polymerase activity. In addition, the extra Hoogsteen base pairs in the CLTAS provide improved affinity and specificity which can be used to identify the single-base mismatch in the target strand.

MATERIALS AND METHODS

Material

All DNA strands were ordered from Sangon Biotech Co., Ltd (Shanghai, China). Unmodified DNA strands were purified by polyacrylamide gel electrophoresis (PAGE), and modified DNA strands with fluorophore and quencher were purified by high-performance liquid chromatography (HPLC). DNA oligonucleotides were dissolved in water as the stock solution and quantified using Nanodrop 2000, and absorption intensities were recorded at $\lambda = 260$ nm. Sequences of all oligonucleotides are listed in Supplementary Table S1. Thermus aquaticus DNA polymerase (Taq DNA polymerase) was purchased from Takara (Takara Biomedical Technology (Beijing) Co., Ltd). Nt. BsmAI, T7 RNA polymerase, dNTP, and rNTP were ordered from New England Biolabs. All other chemicals were of analytical grade and used without further purification.

DNA complexes preparation

The corresponding single strands were mixed in 0.6× RNA Pol reaction buffer (24 mM Tris–HCl, 3.6 mM $MgCl_2$, 0.6 mM DTT, 1.2 mM spermidine, pH 7.9) and annealed in a polymerase chain reaction (PCR) thermal cycler at the reaction condition of decreasing 85°C to 25°C at a rate of −4°C every five minutes and finally kept at 25°C.

DNA polymerase extension and RNA polymerase transcriptional reaction

The reaction mixtures were prepared as part A and part B separately. Part A (total volume of 12.5 μl), including aptamer structure, 50 U/ml Taq DNA polymerase, 0.5 mM dNTPs, 0.6× RNA Pol reaction buffer incubated at 25°C for 30 min. Part B (total volume of 12.5 μl) was composed of 0.6× RNA Pol reaction buffer, 4 U/μl T7 RNA Polymerase, 3 mM rNTP, 40 nM template and 800 nM (1600 nM for gel) reporter probe. Parts A and B were mixed and incubated for gel analysis or put into real-time fluorescence PCR for measuring fluorescence signal. Here, the assessment of the activity of Taq polymerase was conducted at room temperature, where we use 25°C rather than usual elevated temperatures for thermal cycling.

The disassembly of the CLTAS by enzymatic nicking digestion

The triplex aptamer structure incubated with Nt.BsmAI in 0.6× RNA Pol reaction buffer at 37°C for 4 h. Then, the digested product was heated at 80°C for 20 min to deactivate the enzyme. Finally, the product was cooled down to 25°C.

Fluorescent experiments

All experiments were performed in 0.6× RNA Pol reaction buffer using real-time fluorescence PCR (Applied Biosystems, Stepone+). In a typical reaction, the total volume of the solution was 25 μl. The FAM fluorescence was monitored at 2 min intervals. Here, fluorescence data were normalized in the range between 0 and 1. The fluorescence results were obtained by the average values from at least three times repeat experimental results. Unless specifically mentioned, all the experiments were conducted at 25°C.

PAGE experiments

The samples were mixed with 36% glycerin solution and subjected to electrophoresis analysis on a 12% polyacrylamide gel. The analysis was carried out in 1× TAE buffer (40 mM Tris, 20 mM acetic acid, 2 mM EDTA, pH 8.0) supplemented with 12.5 mM $MgCl_2$ at 90 V for 1–2 h at 4°C. After Stains-All (Sigma-Aldrich) or EB (Sangon Biotech) staining, Gels were imaged using scanner or Gel imager (Bio-Rad).

RESULTS AND DISCUSSION

CLTAS mechanism underlying the regulation of DNA polymerase activity

To regulate the activity of Taq polymerase, a strategy based on CLTAS was proposed. The design details of the CLTAS (strand A) are displayed (Figure 1A). It contains three segments: one segment (black hairpin) consists of the conserved sequence of the aptamer which inhibits Taq polymerase activity, and the other two flanking arms (green) are homopyrimidine (TC-rich) sequences separated by the aptamer sequence. The CLTAS acts like an open clamp that cannot bind with Taq polymerase due to the lack of a stable hairpin structure. When the strand Target, the sequences of which are homopurine (AG-rich), is introduced, it binds with the two arms of the CLTAS via Watson–Crick and Hoogsteen base pairings to form a triplex structure, which converts the conformation of the clamp structure from an open state to a closed state. This structural alteration provides the clamp structure with the indispensable hairpin structure for the aptamer. This closed clamp structure binds with Taq polymerase and inhibits its activity. Here, the strand Target has an overhang (red) at the 5′ end for the subsequent strand displacement reaction. Furthermore, to confirm that the suppression of Taq polymerase genuinely results from the triplex structure of the closed CLTAS, we designed duplex-only control aptamer structures, AC1 or AC2, containing one arm with a sequence (green) that was identical to the one in the CLTAS and the other arm with a random sequence (grey) that could not form a triplex.

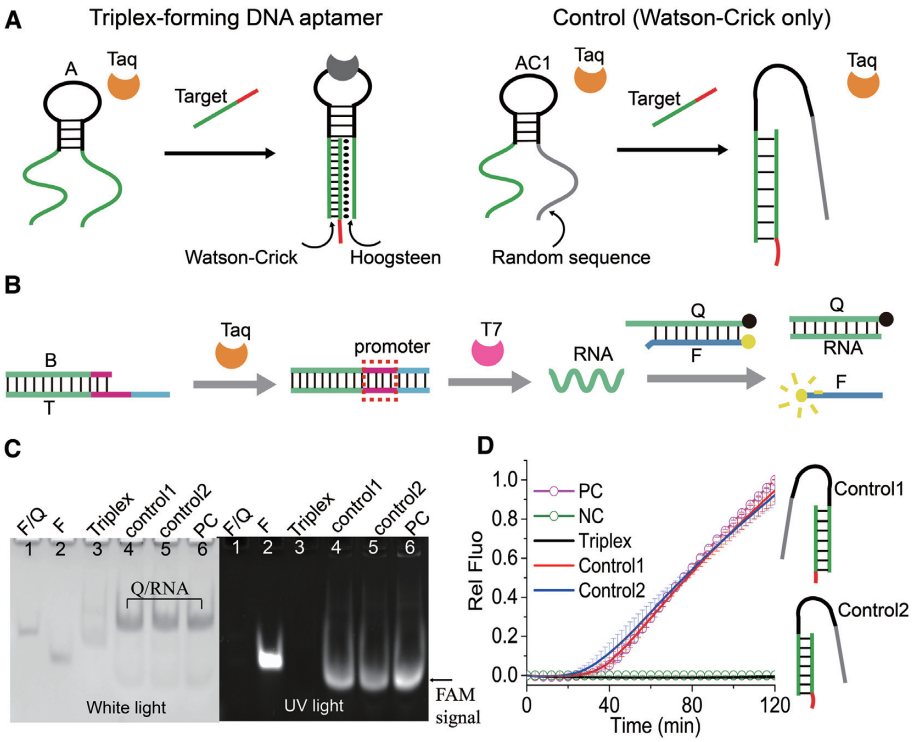

Figure 1. (**A**) Schematic illustration of the CLTAS used to inhibit the activity of Taq polymerase. (**B**) Schematic illustration of the signal transduction unit (STU) that monitors the activity of Taq polymerase via an RNA transcription reaction and a strand displacement reaction. (**C**) Native PAGE (12%) analysis of the inhibitory effect of the CLTAS and the Watson-Crick only aptamers through the STU under white light after staining (left) and UV light without staining (right). (**D**) Results of the fluorescence assay. Triplex consists of a sample containing DNA polymerase and A/Target. Control1(2) contains DNA polymerase and a Watson-Crick only aptamer whose random sequence is located on its two different arms. Control1 corresponds to AC2/EC2 and Control2 AC1/Target. Positive control (PC) contains DNA polymerase. Negative control (NC) does not contain DNA polymerase. [Taq] = 25 U/ml, [A/Target] ([control1(2)]) = 50 nM.

In order to characterize the effect of CLTAS, a signal transduction unit (STU) was designed to convert changes in enzyme activity into RNA transcription events, and then into measurable fluorescent signals (Figure 1B). Briefly, the STU records Taq polymerase activity through a change in the fluorescence signal caused by three reactions, including the primer extension reaction, the RNA transcription reaction, and the displacement reaction. Specifically, the STU is composed of a template (T/B) with an incomplete T7 RNA polymerase promoter sequence and a fluorescent probe F/Q (Supplementary Figure S1). In the active state, DNA polymerase triggers the 5′-3′ extension of T/B and completes the promoter sequence, thus initiating RNA transcription. The transcribed RNA displaces Q from F/Q and generates an increasing fluorescence signal. By contrast, in the inhibited inactive state, the complex T/B cannot serve as the substrate for RNA transcription, thereby preventing enhancement of the fluorescence signal. The introduction of the STU indicates that the CLTAS-based regulation of polymerase activity could be integrated with other nano-systems such as RNA transcription circuits. Moreover, it also suggests that using DNA polymerase as a bridge, the state of *in vitro* transcription (OFF/ON) could be controlled indirectly by the conformational changes of the triplex structure.

Before verifying the feasibility of the CLTAS mechanism of regulating the polymerase activity, the formation of different aptamer structures including the CLTAS (with two 'C' bases in the 12-pair arm stem) and the control structures was examined (Supplementary Figures S2 and S3). The inhibitory effect of these structures towards DNA polymerase was investigated using native PAGE. Introduction of the closed CLTAS (A/Target; left lane 3), did not result in an obvious change in band migration compared to that of the F/Q duplex alone, indicating that Taq polymerase was in a suppressed state and could not initiate the RNA transcription reaction (Figure 1C). In sharp contrast, when either control1 or control2 was present (left lanes 4 and 5), the F/Q band completely disappeared. Accordingly, a new slower-mobility band corresponding to Q/RNA appeared, suggesting that Taq polymerase had not been inhibited and RNA transcription reaction had occurred. In addition, the fact that the bands in lanes 4 and 5 displayed identical migration with the positive control in lane 6 proved that the duplex-only control1 and control2 could not inhibit Taq polymerase activity. To further corroborate the reaction, a FAM-labeled F and a quencher-labelled Q were employed in the gel assay. As expected, in the presence of the triplex structure A/Target (right lane 3), the fluorescence band F was not observed, while upon the addition of control1 or control2, the fluorescence band F appeared clearly, thus confirming that only the closed clamp formed by the triplex aptamer structure could inhibit Taq polymerase. The mechanism of the CLTAS was also monitored using a real-

time fluorescence assay (Figure 1D). When the triplex aptamer structure was introduced, no distinct increase in fluorescence was observed, demonstrating that no significant difference occurred with the negative control, whereas, the sample treated with the control structures produced an intense fluorescence signal whose intensity was nearly the same as that of the positive control. Considered together, these results confirmed the feasibility of the CLTAS.

Parameter analysis of the CLTAS

The inhibitory effect of the CLTAS relies on the stability of the triple-helix aptamer structure. Besides pH, GC content and arm length are also important for the stability of the triplex structure. Considering the near neutral pH conditions required for the DNA polymerase reaction, we adjusted the two parameters, GC content and arm length, in order to inhibit Taq polymerase under fixed pH conditions.

It is known that the triplex C−G·C+ is sensitive to pH and stabilized under acidic conditions, while T−A·T is not sensitive to pH and is relatively stable under neutral conditions (33). In order to study the impact of base composition on inhibitory capability, we designed a series of CLTASs with a fixed arm length of 12 and different GC contents, which possessed 5, 4, 3 and 2 'C' bases, respectively and are referred to as C5, C4, C3 and C2 (Figure 2A). Stability of the above aptamer structures was analyzed using PAGE (Supplementary Figure S4). According to the experimental results, lower GC content was conducive to the formation of the triple helix structure. Thus, C3 and C2 had a higher yield than C5 and C4 under experimental conditions. Since the GC content affected the stability of the triple helix structure, it would also influence the inhibition ability of the CLTAS. As expected, F/Q was consumed upon the addition of C5 and C4 to Taq polymerase (Figure 2B; lanes 2 and 3), followed by the generation of Q/RNA and release of strand F, indicating that unstable C5 and C4 could not inhibit the polymerase. In the presence of C3 (Figure 2B; lane 4), a small amount of F/Q remained unchanged while a majority of F was released, suggesting that as GC content decreased the CLTAS was able to bind a small amount of Taq polymerase. However, when C2 was added (lane 5), the F/Q band did not change and F was not observed, which was attributable to Taq polymerase being completely inhibited by stable C2. Gel results indicated that relatively high GC content led to poor inhibition ability. A real-time fluorescence assay was performed to verify whether the inhibition effect could be induced by CLTASs with different sequences (Figure 2C). The fluorescence intensity of C5 and C4 gradually increased with a faster rate than C3 which lagged for some time. In contrast, C2 led to a significantly reduced fluorescence signal, suggesting its excellent inhibition capability. Therefore, 2 'C' bases were selected for the CLTAS, in subsequent experiments.

In order to examine the effect of arm length on the inhibitory capability of the CLTAS, five aptamer structures containing two 'C' bases and different arm lengths from 8 to 12, referred to as L8, L9, L10, L11 and L12, respectively, were prepared (Figure 3A). After verifying assembly (Supplementary Figure S5 and S18), the inhibitory effect of different arm length toward DNA polymerase was first confirmed using native PAGE (Figure 3B). The gel results showed that L8, L9 and L10 could not inhibit the polymerase and that L11 had a weak capability, while L12 was able to fully bind with the polymerase and inhibit its activity. It was also observed that the fluorescence results in Figure 3C were consistent with those of the gel results. Thus, the CLTAS with two pairs of C−G·C+ and an arm length of 12 could achieve Taq enzyme inhibition under our experimental conditions. A possible reason for the poor inhibition effect of L8–L11 may be that the length of the CLTAS was too short to bind firmly to Taq enzymes. In addition, the CLTAS containing 0 or 1 'C' with an arm length of 10 or 11 bp was also examined (Supplementary Figure S6). The experimental results indicated that even without 'C' base, the CLTAS having a length smaller than 12 could not inhibit polymerase activity. Moreover, when the arm length was prolonged with a fixed GC content (three C–G·C+ base pairings), the CLTAS had a better inhibitory capacity than the one whose arm length was 12 (Supplementary Figure S7).This indicated that, under conditions of a fixed GC content, the inhibitory capacity of the aptamer may be enhanced by extending the arm length of the CLTAS. Thereby, the inhibition capacity of the CLTAS could be dynamically regulated by tuning GC content and arm length of the triple-helix. Such programmability constitutes an important advantage displayed by CLTAS over other non-triple helix structures. As a biosensing application of the CLTAS, a DNA detecting network that can recognize the BRCA1 gene fragment was constructed (Supplementary Figure S15).

Conformation of the CLTAS also affected its repression effect on DNA polymerase. The CLTASs with an overhang on different terminals of the strand Target were explored. It was found that the CLTAS with a 5′ overhang was able to inhibit DNA polymerase, while the one with a 3′ overhang could not (Supplementary Figure S8). A possible reason for this may be that the overhang of the latter was near to the conserved sequence-formed loop, which was not conducive to binding between the polymerase and the aptamer structure.

Based on these experimental results, an arm length of 12 in combination with two C−G·C+ base pairs and a strand Target with an overhang far from the loop, was chosen as the CLTAS for the experiments that followed.

In order to fine tune the regulation of polymerase activity, various concentrations of the strand Target (5, 10, 20, 30, 40, 50 nM) were assessed by monitoring changes in the fluorescence signal. The final fluorescence intensity increased as Target concentrations decreased from 40 to 5 nM, thereby substantiating the finding that higher Target concentrations enhanced the inhibition of Taq polymerase, which resulted in less fluorescent strand F being released (Figure 4). When the Target concentration was 50 nM, fluorescence intensity remained almost unchanged, indicating that Taq polymerase was fully inhibited. Thus, 50 nM CLTAS was employed to suppress 25 U/ml Taq polymerase in subsequent experiments.

To compare the inhibition effect of the CLTAS and the duplex aptamer structures (14), a control experiment was performed. The triplex aptamer structure, A/Target, and the duplex aptamer structure, D/Target were prepared (Fig-

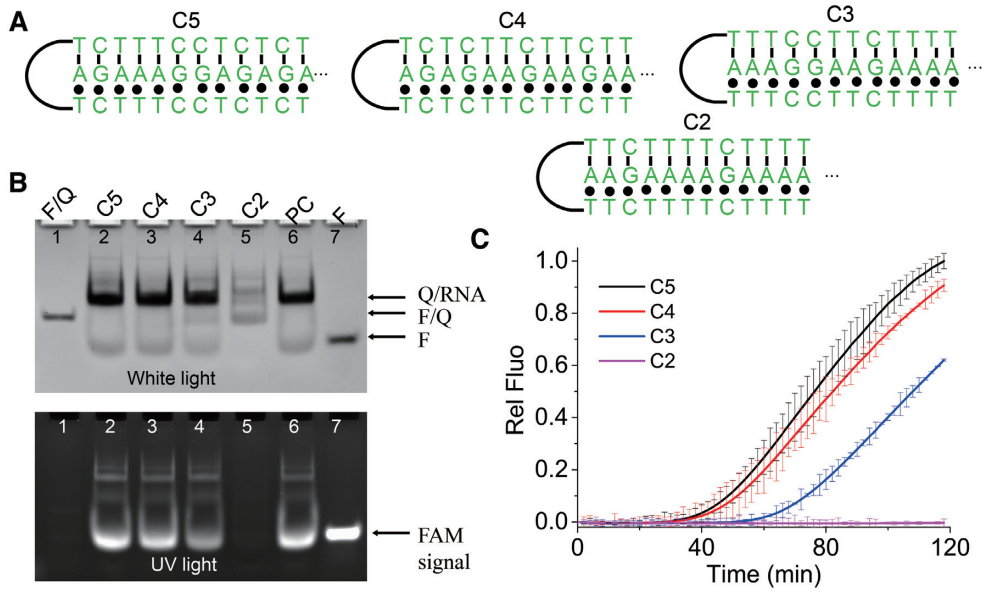

Figure 2. (**A**) CLTAS with different GC contents in the arm. C*i* (*i* = 5, 4, 3, 2) represents the assembled structure, where number of 'C' bases in the arm sequence is *i*, respectively. (**B**) Native PAGE (12%) analysis of the inhibitory effect of Ci under white light after staining (top) and UV light without staining (bottom). (**C**) Results of the fluorescence assay. C*i* is a sample consisting of DNA polymerase and corresponding complexes, respectively. [Taq] = 25 U/ml, [C*i*] = 50 nM.

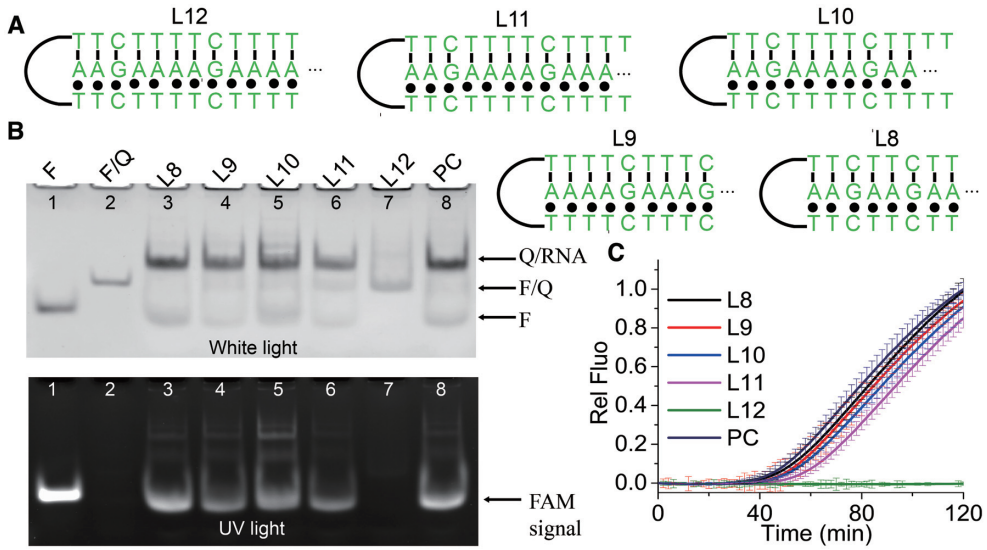

Figure 3. (**A**) CLTAS with different arm lengths. L*i* (*i* = 8, 9, 10, 11, 12) represents the assembled structure the arm length of which was *i*, respectively. (**B**) Native PAGE (12%) analysis of the inhibitory effect of L*i* under white light after staining (top) and UV light without staining (bottom). (**C**) Results of the fluorescence assay. L*i* is a sample consisting of DNA polymerase and corresponding complexes, respectively. [Taq] = 25 U/ml, [L*i*] = 50 nM.

ure 5A). They contained the same conserved aptamer sequence (black), where the former had two arms (green) while the latter had only one. The fluorescent signal corresponding to the duplex (red curve) began to increase while that of the triplex (black curve) remained unchanged during the reaction (Figure 5B). According to these results, the triplex aptamer had a stronger inhibition effect than that of the duplex. The reason for this may be that the extra Hoogsteen base pairings of the triplex accounted for a more stable structure than the duplex.

Distinguishing single-base mismatches based on CLTAS

The CLTAS recognizes its target through Watson-Crick and Hoogsteen base pairings, which provides an enhanced affinity and greater discrimination efficiency. To verify its discrimination capability, the CLTAS was employed to detect a single-base mismatch. A series of strands with one mismatch at different positions, M3, M4, M5, M8 and M10, were designed (Figure 6A). The mismatched targets had the same sequence as that of the fully matched target except for a mutated base in the corresponding position (e.g. some 'A'

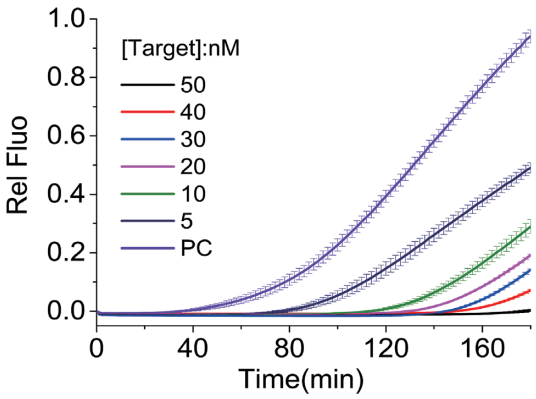

Figure 4. Fluorescence results of the CLTAS with different target concentrations through the STU. [Taq] = 25 U/ml, [A] = 50 nM.

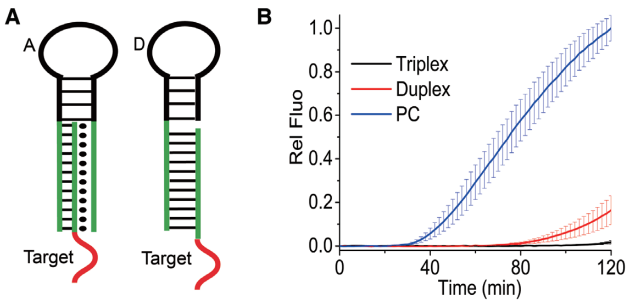

Figure 5. (**A**) Schematic diagram of the CLTAS and the double-helix aptamer structure. (**B**) Time-dependent fluorescence intensity analysis of triplex-induced and duplex-induced suppression of DNA polymerase through the STU. [Taq] = 25 U/ml, [A/Target] ([D/Target]) = 50 nM.

or 'G' base was substituted with a 'C' base). Formation of the aptamer structures with a mismatch was analysed first (Supplementary Figure S9). Next, a fluorescence assay was conducted in order to detect differences between the fully matched target and strands with a single-base mismatch. The mismatched samples produced strong fluorescent signals while the perfectly matched sample generated a significantly low fluorescent signal (Figure 6B). PAGE results further corroborated the above conclusion. Similar to th e positive control, the disappearance of the F/Q band accompanied by the appearance of the Q/RNA band and F in lane 5, 6, 7, 8, 9, indicated that an aptamer structure with a mismatch was unable to inhibit the DNA polymerase (Figure 6C). By contrast, the intact F/Q in lane 3 suggested that the perfectly matched target had a strong inhibitory effect. In addition to the mismatched strands shown (Figure 6A), other mismatched strands at other positions adjacent to the ends were also examined (Supplementary Figures S10 and S11), suggesting that the CLTAS could distinguish single-base mismatches at different positions. Thus, the CLTAS demonstrated excellent ability to distinguish single-base mismatches.

Activation of the DNA polymerase by displacement reaction based on CLTAS

Inhibition of Taq polymerase by the CLTAS depends on the conformation of the triplex structure. Thus, regulation could be further implemented by reconfiguring the triplex aptamer via auxiliary triggers, such as DNA strands, RNA strands or enzymes. DNA strand displacement is an effective means to achieve conformational changes due to its robust and modular properties. Here, strand displacement reaction was employed to disrupt the triplex structure. Initially, the DNA polymerase was captured by the CLTAS in the suppressed inactive state (Figure 7A). Introduction of the complementary strand C displaced the Target and facilitated their hybridization to form a duplex. Therefore, disassembly of the triplex structure resulted in the release of Taq polymerase.

We first explored the feasibility of strand displacement based on the triplex structure. It was observed that the displacement occurred under our experimental conditions (Supplementary Figure S12). Then, activation of Taq polymerase using the strand displacement reaction was measured using a fluorescence assay and PAGE. Fluorescence intensity increased upon the addition of strand C (red curve; Figure 7B), indicating the disassembly of CLTAS. It was noteworthy that there was a lag in the increase of the fluorescence signal relative to that of the positive control. This could be attributed to the displacement reaction which takes some time. By contrast, the fluorescence signal remained unchanged in the absence of C (black curve; Figure 7B) during the reaction, suggesting that the triplex structure was intact. Gel electrophoresis further confirmed the switching of the polymerase. In the absence of strand C, the F band did not appear (Figure 7C; lane 2). Conversely, F/Q disappeared and F appeared upon the addition of strand C (Figure 7C; lane 3). These results demonstrated that similar to the duplex aptamer structure, the triplex structure could also tune the activity of Taq polymerase via the strand displacement reaction. Besides, NOT and YES logic circuits that could recognize the DNA strand were constructed based on the above reaction (Supplementary Figures S16 and S17).

Activation of the DNA polymerase by enzymatic nicking digestion based on CLTAS

Apart from the displacement reaction, digestion by the nicking enzyme also achieved disassembly of the duplex structure. We surmised that this strategy could be applied to the triplex aptamer structure by incorporating the recognition sequence of the nicking enzyme into the triplex arm. Here, Nt.BsmAI was employed to disrupt the triplex structure. The conserved sequence, 5′-GTCTCNN-3′ (N being a variable nucleotide), of Nt.BsmAI was inserted into one arm of AN and the bases of 'NN' was replaced by 'TT' (Figure 8A). There was a six-base overlap between the triplex and the enzyme recognition site. In this manner, not only the requirement of the formation of the triplex structure but also the recognition site of the nicking enzyme was satisfied. Due to the action of Nt.BsmAI, one triplex arm was cleaved and the triplex structure became unstable. This, in turn, led to the release of strand EN from the unstable complex and resulted in the disassembly of the triplex structure. Therefore, Taq polymerase was released and activated.

In order to achieve enzymatic digestion-induced activation of DNA polymerase, two control experiments were

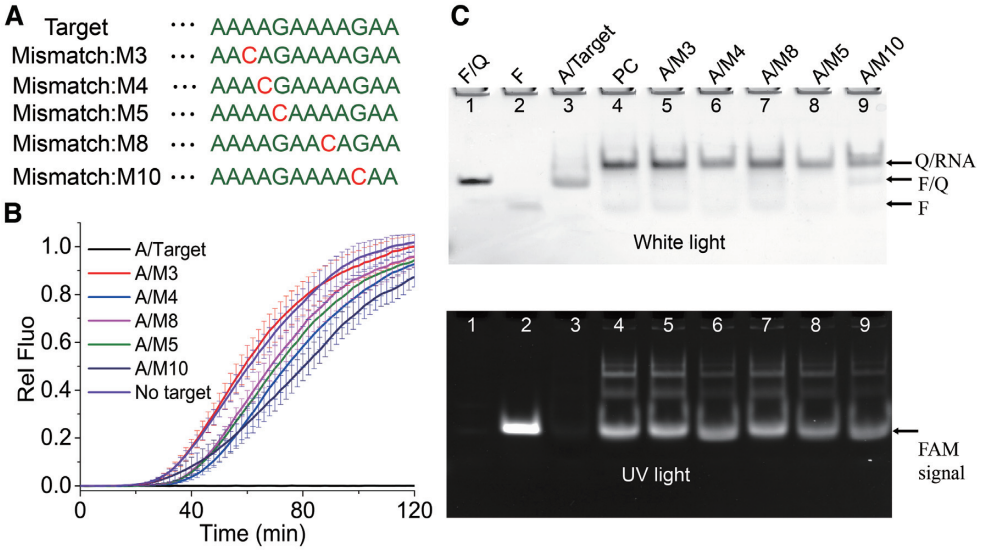

Figure 6. (**A**) DNA sequence of fully matched Target and the strand with a single-base mismatch. (**B**) Fluorescence analysis of the inhibitory effect of the CLTAS with a fully matched Target or a single-base mismatch strand. (**C**) Native PAGE (12%) analysis under white light after staining (top) and UV light without staining (bottom). A/Target or A/M*i* (*i* = 3, 4, 5, 8, 10) is a sample consisting of DNA polymerase and corresponding complexes, respectively. [Taq] = 25 U/ml, [A/Target] ([A/M*i*]) = 50 nM.

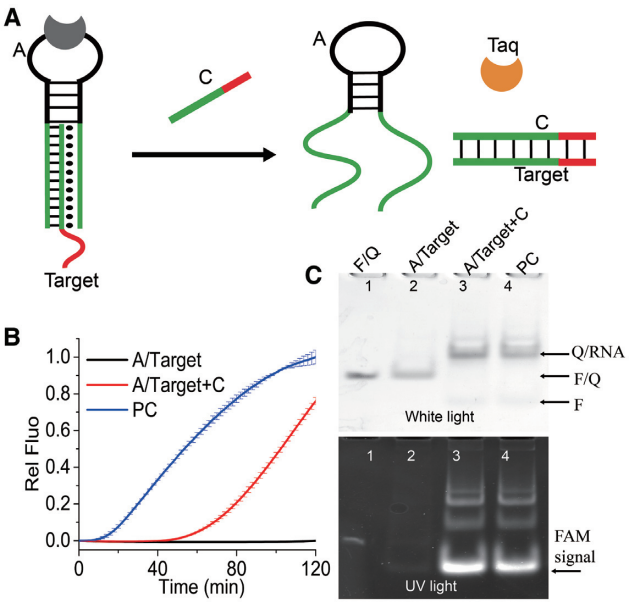

Figure 7. (**A**) Schematic of polymerase release from triplex-forming aptamer via strand displacement reaction. (**B**) Fluorescence results of displacement-induced activation of DNA polymerase. (**C**) Native PAGE (12%) results under white light after staining (top) and UV light without staining (bottom). A/Target, A/Target + C are samples without or with complementary strand C in the presence of DNA polymerase. Positive control (PC) is a sample containing DNA polymerase. [Taq] = 25 U/ml, [A/Target] = 50 nM, [C] = 50 nM.

performed to test the feasibility of the design: one verified whether the designed CLTAS preserved an affinity towards Taq polymerase, and the other verified whether the designed CLTAS could be digested by Nt.BsmAI. We confirmed that the designed CLTAS was able to inhibit the DNA polymerase (Supplementary Figure S13). Besides, we also designed a control structure, ANC/EN, that contained only a double helix structure, to confirm that the inhibitory effect was indeed caused by the triple-helix aptamer structure (Supplementary Figure S13). Previous studies had shown that triplex formation would effectively inhibit specific protein–DNA interactions and thus suppress the enzymatic digestion and modification (26). Thereby, we verified whether the designed CLTAS could be cleaved under the action of Nt.BsmAI. As opposed to previous studies, the aptamer structure in our design was cleaved by the nicking enzyme and the digestion also worked well in a polymerase reaction buffer (Supplementary Figure S14). The successful operation of the nicking enzyme may be attributed to the following two reasons. One possible reason might be that Nt.BsmAI belongs to a type of endonuclease that cleaves only one DNA strand of the substrate, while those enzymes inhibited by triplex structures, such as EcoRI (26) are restriction endonucleases that cleave both the two strands of the substrate. The other possible reason might be that the CLTAS had a hairpin structure different from those linear triplex structures.

A fluorescence experiment and gel electrophoresis were performed to explore Taq polymerase activation by the nicking enzyme. The CLTAS treated with Nt.BsmAI gave rise to an intense fluorescence signal which was comparable to that of the positive control, while fluorescence inte nsity remained unchanged in the absence of the nicking enzyme (Figure 8B), indicating that the nicking enzyme had activated DNA polymerase. Furthermore, the gel results also confirmed the effectiveness of the nicking enzyme-induced switching of DNA polymerase activity (Figure 8C). In addition, a YES logic circuit that could recognize the nicking enzyme was established based on the above reaction (Supplementary Figure S17).

In general, similar to the double-helix aptamer structure, the triple-helix structure could also activate Taq poly-

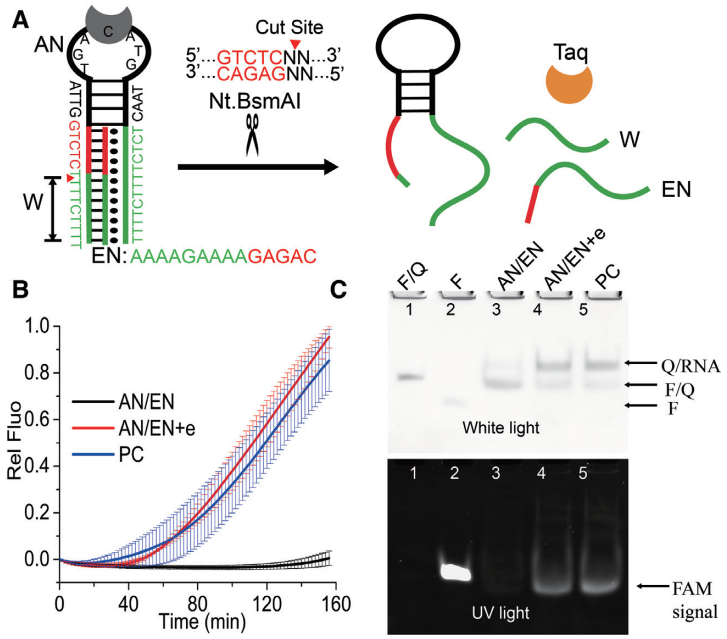

Figure 8. (**A**) Schematic showing release of polymerase from the triplex-forming aptamer via enzymatic nicking digestion. (**B**) Fluorescence results of the digestion-induced activation of DNA polymerase. (**C**) Native PAGE (12%) results under white light after staining (top) and UV light without staining (bottom). AN/EN, AN/EN + e are samples without or with nicking enzyme in the presence of DNA polymerase. [Taq] = 25 U/ml, [AN/EN] = 50 nM, [Nt.BsmAI] = 0.1 U/μl.

merase when the appropriate nicking enzyme was selected to change the conformation.

CONCLUSIONS

In our study, a triplex-based approach was presented to regulate the activity of DNA polymerase. This strategy incorporates the aptamer sequence into a clamp-like triplex structure. In order to achieve good inhibition capability, CLTASs with different arm lengths and base compositions were explored. The CLTAS recognized its target through the interaction of Watson–Crick and Hoogsteen, which provided enhanced affinity and greater discrimination efficiency. To demonstrate this process, we utilized the CLTAS to identify a single-base mismatch in the target strand. Although the conformation of the CLTAS is different from that of duplex structures, it can be altered by applying a similar operation to the double helix structure. In order to demonstrate this, allostery of the CLTAS, which was realized by a strand displacement reaction and nicking enzyme digestion, was employed to regulate the activity of Taq polymerase.

Until now, the triplex structure has been used to function as aptasensors. However, the design in our strategy is completely distinct from those aptasensors that are based on the triple helix molecular switch, which detects target molecules by releasing the aptamer, thereby causing a conformational change (24). The triple helical structure here serves as a part of the aptamer structure. Our design is also different from those aptasensors that employs triple helical structures to fix the aptamer to improve its structural stability (50), because the triple helical structure (50) is used only as an auxiliary element of the aptamer structure. Moreover, there have been efforts to regulate the activity of polymerases and ribozymes (51,52) via the triplex clamp. However, the regulatory mechanism of polymerase activity (51,52) is distinct from ours, the former achieves the inhibition by blocking protein–DNA interactions through the triplex structure, while our strategy is realized by facilitating the binding of polymerase with the triplex structure. Compared with the method using acyclic (L)-threoninol nucleic acid (aTNA) and the artificial nucleic acids (51), the sequence of CLTAS is free of artificial nucleic acids, which makes the synthesis of the sequence convenient. Moreover, these two approaches could couple well to set up more complex control systems such as AND logic by recovering polymerase activity with the proposed approach and obtaining available substrates with the method (51).

In summary, the proposed strategy in our work, which combines the advantages of both aptamer and triplex structures, exhibits excellent specificity and discrimination efficiency resulting in an ability to distinguish single-base mismatches. On one hand, the CLTAS demonstrates a stronger inhibition ability than that of its corresponding duplex due to its high affinity. On the other hand, the inhibitory capability of the CLTAS can be adjusted by altering the relative content of T-A·T/C−G·C+ triplets, by varying the arm length or by incorporating a triplex intercalator (31). Thus, it provides a flexible, programmable, and controllable way to regulate the activity of DNA polymerase. In addition, the CLTAS could be used in conjunction with other polymerases provided they have stem–loop aptamers amenable to triplex-mediated switching, thus broadening the utility of the method. As demonstrated in supplementary information S7, the CLTAS strategy expands the toolbox of DNA nanotechnology and shows potential in the areas

of biosensing, biocomputing and programmable nanomachines.

SUPPLEMENTARY DATA

Supplementary Data are available at NAR Online.

FUNDING

National Key R&D Program of China for International S&T Cooperation Projects [2017YFE0103900]; National Natural Science Foundation of China [61772214]. Funding for open access charge: National Key R&D Program of China for International S&T Cooperation Projects [2017YFE0103900].
Conflict of interest statement. None declared.

REFERENCES

1. Goodey,N.M. and Benkovic,S.J. (2008) Allosteric regulation and catalysis emerge via a common route. *Nat. Chem. Biol.*, **4**, 474–482.
2. Harroun,S.G., Prevost-Tremblay,C., Lauzon,D., Desrosiers,A., Wang,X., Pedro,L. and Vallee-Belisle,A. (2018) Programmable DNA switches and their applications. *Nanoscale*, **10**, 4607–4641.
3. Nutiu,R. and Li,Y. (2003) Structure-switching signaling aptamers. *J. Am. Chem. Soc.*, **125**, 4771.
4. Bonham,A.J., Hsieh,K., Ferguson,B.S., Vallee-Belisle,A., Ricci,F., Soh,H.T. and Plaxco,K.W. (2012) Quantification of transcription factor binding in cell extracts using an electrochemical, structure-switching biosensor. *J. Am. Chem. Soc.*, **134**, 3346–3348.
5. Zhu,G.Z., Zhang,S.F., Song,E.Q., Zheng,J., Hu,R., Fang,X.H. and Tan,W.H. (2013) Building fluorescent DNA Nanodevices on target living cell surfaces. *Angew Chem Int Edit*, **52**, 5490–5496.
6. Tintore,M., Gallego,I., Manning,B., Eritja,R. and Fabrega,C. (2013) DNA origami as a DNA repair nanosensor at the single-molecule level. *Angew. Chem.*, **52**, 7747–7750.
7. Chakraborty,K., Veetil,A.T., Jaffrey,S.R. and Krishnan,Y. (2016) Nucleic acid-based nanodevices in biological imaging. *Annu. Rev. Biochem.*, **85**, 349–373.
8. Liang,H., Chen,S., Li,P., Wang,L., Li,J., Li,J., Yang,H.H. and Tan,W. (2018) Nongenetic approach for imaging protein dimerization by aptamer recognition and proximity-induced DNA assembly. *J. Am. Chem. Soc.*, **140**, 4186–4190.
9. Li,L., Chen,X., Cui,C., Pan,X., Li,X., Yazd,H.S., Wu,Q., Qiu,L., Li,J. and Tan,W. (2019) Aptamer displacement reaction from live-cell surfaces and its applications. *J. Am. Chem. Soc.*, **141**, 17174–17179.
10. Peng,R., Zheng,X., Lyu,Y., Xu,L., Zhang,X., Ke,G., Liu,Q., You,C., Huan,S. and Tan,W. (2018) Engineering a 3D DNA-logic gate nanomachine for bispecific recognition and computing on target cell surfaces. *J. Am. Chem. Soc.*, **140**, 9793–9796.
11. X,C., C,Z., C,L., Y,S., M,Z., Y,Z., L,Y., D,H. and W,T. (2019) Construction of a multiple-aptamer-based DNA logic device on live cell membranes via associative toehold activation for accurate cancer cell identification. *J. Am. Chem. Soc.*, **141**, 12738–12743.
12. Lin,Y. and Jayasena,S.D. (1997) Inhibition of multiple thermostable DNA polymerases by a heterodimeric aptamer 1. *J. Mol. Biol.*, **271**, 100–111.
13. Ohuchi,S., Mori,Y. and Nakamura,Y. (2012) Evolution of an inhibitory RNA aptamer against T7 RNA polymerase. *FEBS Open Biol.*, **2**, 203.
14. Park,K.S., Lee,C.Y. and Park,H.G. (2015) Target DNA induced switches of DNA polymerase activity. *Chem. Commun.*, **51**, 9942–9945.
15. Park,K.S., Lee,C.Y. and Park,H.G. (2016) Metal ion triggers for reversible switching of DNA polymerase. *Chem. Commun.*, **52**, 4868–4871.
16. Wang,Z., Li,Y., Han,P., Mao,X., Yin,Y. and Cao,Y. (2016) Binding-responsive catalysis of Taq DNA polymerase for the sensitive and selective detection of cell-surface proteins. *Chem. Commun.*, **52**, 10684–10687.
17. Huang,Y., Li,H., Wang,L., Mao,X.X. and Li,G.X. (2016) Highly sensitive protein detection based on smart hybrid nanocomposite-controlled switch of DNA polymerase activity. *ACS Appl. Mater. Interfaces*, **8**, 28202–28207.
18. Jung,Y.J., Lee,C.Y., Park,K.S. and Park,H.G. (2019) Sensitive and specific detection of proteins based on target-responsive DNA polymerase activity. *Anal. Chim. Acta*, **1059**, 80–85.
19. Park,K.S., Lee,C.Y., Kang,K.S. and Park,H.G. (2017) Aptamer-mediated universal enzyme assay based on target-triggered DNA polymerase activity. *Biosens. Bioelectron.*, **88**, 48–54.
20. Jung,Y., Lee,C.Y., Park,K.S. and Park,H.G. (2019) Target-activated DNA polymerase activity for sensitive RNase H activity assay. *Biotechnol. J.*, **14**, 1800645.
21. Pan,L., Hu,Y., Ding,T., Xie,C., Wang,Z., Chen,Z., Yang,J. and Zhang,C. (2019) Aptamer-based regulation of transcription circuits. *Chem. Commun.*, **55**, 7378–7381.
22. Chandrasekaran,A.R. and Rusling,D.A. (2018) Triplex-forming oligonucleotides: a third strand for DNA nanotechnology. *Nucleic Acids Res.*, **46**, 1021–1037.
23. Hu,Y.W., Cecconello,A., Idili,A., Ricci,F. and Willner,I. (2017) Triplex DNA nanostructures: from basic properties to applications. *Angew Chem Int Edit*, **56**, 15210–15233.
24. Bagheri,E., Abnous,K., Alibolandi,M., Ramezani,M. and Taghdisi,S.M. (2018) Triple-helix molecular switch-based aptasensors and DNA sensors. *Biosens. Bioelectron.*, **111**, 1–9.
25. Vasquez,K.M., Narayanan,L. and Glazer,P.M. (2000) Specific mutations induced by triplex-forming oligonucleotides in mice. *Science*, **290**, 530–533.
26. Hanvey,J.C., Shimizu,M. and Wells,R.D. (1990) Site-specific inhibition of EcoRI restriction/modification enzymes by a DNA triple helix. *Nucleic Acids Res.*, **18**, 157–161.
27. Zhou,Z., Giles,K.E. and Felsenfeld,G. (2019) DNA center dot RNA triple helix formation can function as a cis-acting regulatory mechanism at the human beta-globin locus. *Proc. Natl. Acad. Sci. U.S.A.*, **116**, 6130–6139.
28. Grossmann,T.N., Roglin,L. and Seitz,O. (2007) Triplex molecular beacons as modular probes for DNA detection. *Angew. Chem. Int. Ed.*, **46**, 5223–5225.
29. Lu,S., Wang,S., Zhao,J., Sun,J. and Yang,X. (2018) Classical triplex molecular beacons for MicroRNA-21 and vascular endothelial growth factor detection. *ACS Sens*, **3**, 2438–2445.
30. Guo,B.Y., Sheng,Y.Y., Zhou,K., Liu,Q.S., Liu,L. and Wu,H.C. (2018) Analyte-Triggered DNA-Probe release from a triplex molecular beacon for nanopore sensing. *Angew. Chem. Int. Ed.*, **57**, 3602–3606.
31. Wang,J., Li,T.T., Li,H.G., Li,G.K., Wu,S.X. and Ling,L.S. (2019) A universal colorimetric PCR biosensor based upon triplex formation with the aid of Ru(phen)(2)dppx(2+). *Sens. Actuators B-Chem.*, **278**, 39–45.
32. Del Grosso,E., Idili,A., Porchetta,A. and Ricci,F. (2016) A modular clamp-like mechanism to regulate the activity of nucleic-acid target-responsive nanoswitches with external activators. *Nanoscale*, **8**, 18057–18061.
33. Idili,A., Vallee-Belisle,A. and Ricci,F. (2014) Programmable pH-triggered DNA nanoswitches. *J. Am. Chem. Soc.*, **136**, 5836–5839.
34. Patino,T., Porchetta,A., Jannasch,A., Llado,A., Stumpp,T., Schaffer,E., Ricci,F. and Sanchez,S. (2019) Self-sensing enzyme-powered micromotors equipped with pH-Responsive DNA nanoswitches. *Nano Lett.*, **19**, 3440–3447.
35. Idili,A., Plaxco,K.W., Vallee-Belisle,A. and Ricci,F. (2013) Thermodynamic basis for engineering high-affinity, high-specificity binding-induced DNA clamp nanoswitches. *Acs Nano*, **7**, 10863–10869.
36. Chen,X.X., Chen,T.S., Ren,L.J., Chen,G.F., Gao,X.H., Li,G.X. and Zhu,X.L. (2019) Triplex DNA nanoswitch for pH-Sensitive release of multiple cancer drugs. *ACS Nano*, **13**, 7333–7344.
37. Han,X.G., Zhou,Z.H., Yang,F. and Deng,Z.X. (2008) Catch and release: DNA tweezers that can capture, hold, and release an object under control. *J. Am. Chem. Soc.*, **130**, 14414-+.
38. Ranallo,S., Prevost-Tremblay,C., Idili,A., Vallee-Belisle,A. and Ricci,F. (2017) Antibody-powered nucleic acid release using a DNA-based nanomachine. *Nat. Commun.*, **8**, 15150.
39. Yang,S.S., Jiang,M.H., Chai,Y.Q., Yuan,R. and Zhuo,Y. (2018) Application of Antibody-Powered Triplex-DNA nanomachine to electrochemiluminescence biosensor for the detection of

anti-digoxigenin with improved sensitivity versus cycling strand displacement reaction. *ACS Appl. Mater. Interfaces*, **10**, 38648–38655.
40. Yao,D.B., Li,H., Guo,Y.J., Zhou,X., Xiao,S.Y. and Liang,H.J. (2016) A pH-responsive DNA nanomachine-controlled catalytic assembly of gold nanoparticles. *Chem. Commun.*, **52**, 7556–7559.
41. Chen,Y., Lee,S.H. and Mao,C. (2004) A DNA nanomachine based on a duplex-triplex transition. *Angew. Chem. Int. Ed.*, **43**, 5335–5338.
42. Mariottini,D., Idili,A., Vallee-Belisle,A., Plaxco,K.W. and Ricci,F. (2017) A DNA nanodevice that loads and releases a cargo with hemoglobin-like allosteric control and cooperativity. *Nano Lett.*, **17**, 3225–3230.
43. Kuzyk,A., Urban,M.J., Idili,A., Ricci,F. and Liu,N. (2017) Selective control of reconfigurable chiral plasmonic metamolecules. *Sci. Adv.*, **3**, e1602803.
44. Wu,N. and Willner,I. (2016) pH-Stimulated reconfiguration and structural isomerization of origami dimer and trimer systems. *Nano Lett.*, **16**, 6650–6655.
45. Hu,Y., Ren,J., Lu,C.H. and Willner,I. (2016) Programmed pH-Driven reversible association and dissociation of interconnected circular DNA dimer nanostructures. *Nano Lett.*, **16**, 4590–4594.
46. Liao,W.C., Riutin,M., Parak,W.J. and Willner,I. (2016) Programmed pH-responsive microcapsules for the controlled release of CdSe/ZnS quantum dots. *ACS Nano*, **10**, 8683–8689.
47. Kahn,J.S., Freage,L., Enkin,N., Garcia,M.A.A. and Willner,I. (2017) Stimuli-responsive DNA-functionalized metal-organic frameworks (MOFs). *Adv. Mater.*, **29**, doi: 10.1002/adma.201602782.
48. Lu,S.S., Wang,S., Zhao,J.H., Sun,J. and Yang,X.R. (2018) A pH-controlled bidirectionally pure DNA hydrogel: reversible self-assembly and fluorescence monitoring. *Chem. Commun.*, **54**, 4621–4624.
49. Ottaviani,A., Iacovelli,F., Idili,A., Falconi,M., Ricci,F. and Desideri,A. (2018) Engineering a responsive DNA triple helix into an octahedral DNA nanostructure for a reversible opening/closing switching mechanism: a computational and experimental integrated study. *Nucleic Acids Res.*, **46**, 9951–9959.
50. Zhao,L., Qi,X., Yan,X., Huang,Y., Liang,X., Zhang,L., Wang,S. and Tan,W. (2019) Engineering aptamer with enhanced affinity by triple helix-based terminal fixation. *J. Am. Chem. Soc.*, **141**, 17493–17497.
51. Gothelf,K.V. (2019) Toehold-mediated strand displacement in a triplex forming nucleic acid clamp for reversible regulation of polymerase activity and protein expression. *Chemistry*, **25**, 12303–12307.
52. Xia,X., Piao,X.J. and Bong,D. (2014) Bifacial peptide nucleic acid as an allosteric switch for aptamer and ribozyme function. *J. Am. Chem. Soc.*, **136**, 7265–7268.